Université de Montréal

**Nucléation de nanobulles dans le silicium
et piégeage d'impuretés métalliques**

par

Carl Wintgens

Département de physique

Faculté des arts et des sciences

Mémoire présenté à la Faculté des études supérieures
en vue de l'obtention du grade de
Maître ès sciences (M.Sc.)
en Physique

Février 2000

© Carl Wintgens, 2000

Université de Montréal
Faculté des études supérieures

Ce mémoire intitulé :

**Nucléation de nanobulles dans le silicium
et piégeage d'impuretés métalliques**

présenté par :

Carl Wintgens

a été évalué par un jury composé des personnes suivantes :

MM. Robert W. Cochrane, président-rapporteur
Sjoerd Roorda, directeur de recherche
Ludvik Martinu, membre du jury

Mémoire accepté le : _____

*I was born not knowing and have only had
a little time to change that here and there.*

Richard P. Feynman

SOMMAIRE

Ce mémoire est constitué de deux articles ayant comme sujet d'étude principal les cavités de quelques nanomètres de diamètre formées dans le silicium par implantation d'hélium ou d'hydrogène à haute dose et recuit à haute température. Le premier article porte sur le piégeage d'impuretés métalliques sur les parois de ces cavités. Dans cet article, nous voulons connaître l'influence de la taille des nanocavités sur l'efficacité de piégeage d'impuretés d'or. Plus précisément, nous voulons déterminer l'effet de la courbure des cavités sur le potentiel chimique d'atomes d'or piégés à leurs surfaces. Théoriquement, nous nous attendons à ce que l'énergie de piégeage de l'or adsorbé à la surface des plus petites cavités soit plus grande dû à une plus grande courbure de leur surface. Pour vérifier cette hypothèse expérimentalement, nous observons le transport et le piégeage d'or initialement contenu dans une couche de nanocavités relativement grandes vers une couche de petites cavités lors d'un recuit à haute température. Lorsque l'équilibre est atteint, le rapport des quantités d'or par unité de surface contenues dans chacune des couches permet de déterminer la différence d'énergie de piégeage entre les petites et grandes nanocavités. Nous observons que des cavités de 12 nm de diamètre sont quatre fois plus efficaces que des cavités de 34 nm pour le piégeage d'impuretés d'or. Nous comparons ensuite ce résultat avec la valeur théorique obtenue en tenant compte des effets de courbure. Nous proposons également des effets de reconstruction de surface pour expliquer l'efficacité de piégeage des plus petites nanocavités.

Dans le second article, nous nous intéressons au processus de formation des nanobulles dans le silicium. Nous recherchons les doses critiques nécessaires à la création de nanocavités par co-implantation d'hydrogène et d'hélium. L'hydrogène et l'hélium ont des comportements très différents lorsque implantés dans le silicium : l'hydrogène réagit avec les liens brisés de silicium créés durant l'implantation tandis que l'hélium a tendance à précipiter en amas dû à sa solubilité extrêmement faible dans le silicium. Nous voulons donc combiner les effets de l'hydrogène et de l'hélium de façon à optimiser la formation de nanocavités. La création de cavités est indirectement observée par la diffusion et le piégeage d'atomes d'or intentionnellement introduits dans le silicium. Une technique sensible aux défauts de type lacune est également utilisée pour confirmer la présence de nanocavités. Nous montrons que l'implantation de quantités égales d'hydrogène et d'hélium permet de diminuer la dose critique de près d'un facteur trois comparée à une implantation d'hydrogène seulement. Nous présentons finalement un modèle de nucléation de nanobulles, précurseurs des nanocavités. La présence des nanobulles après implantation est une condition nécessaire à la formation de nanocavités lors du recuit à haute température. Le modèle permet de calculer les quantités critiques d'hydrogène et d'hélium requises pour la création de nanobulles dans le silicium. Selon ce modèle, l'efficacité de la co-implantation est due à une diminution de l'énergie libre de surface causée par la passivation des liens pendants de silicium par l'hydrogène.

TABLE DES MATIÈRES

INTRODUCTION

L'implantation d'hélium dans le silicium à température ambiante et à haute dose produit des bulles de quelques nanomètres de diamètre. Ces bulles d'hélium sont observées lorsqu'une dose critique de 10^{16} He/cm^2 est atteinte, indépendamment de l'énergie d'implantation. Par la suite, un traitement thermique à haute température permet aux bulles de croître et à l'hélium de diffuser à travers la matrice pour ensuite s'évaporer à la surface de l'échantillon, laissant dans le silicium des bulles vides de 5-100 nm de diamètre. La surface de ces cavités, non-oxydée et parfaitement propre, est d'un grand intérêt pour la recherche fondamentale et appliquée.

En 1993, Myers *et al.*[1] ont démontré que ces nanocavités représentent des sites très efficaces pour le piégeage d'impuretés métalliques. Ces impuretés, même présentes sous forme de traces, peuvent être hautement nuisibles au fonctionnement des dispositifs microélectroniques. Les niveaux électroniques profonds associés à la présence de celles-ci favorisent la recombinaison de paires électron-trou et sont à l'origine de la diminution du temps de vie des porteurs de charge dans les transistors. De plus, les impuretés métalliques peuvent précipiter dans les régions critiques des dispositifs menant au claquage de ces derniers. En conséquence, le contenu en impuretés métalliques suggéré par la *Semiconductor Industry Association* est aussi bas que 2.5×10^9 atomes/cm^2 dans le cas de

---

[1] S.M. Myers, D.M. Bishop, D.M. Follstaedt, H.J. Stein, et W.R. Wampler, Mater. Res. Soc. Symp. Proc. **283**, 549 (1993).

mémoires à haute densité.[2]

Les méthodes de piégeage généralement utilisées par les manufacturiers pour diminuer les concentrations d'impuretés métalliques dans les dispositifs consistent à former des précipités de siliciure de métal dans une région d'imperfections créée à l'endos de la gaufre. La supériorité du piégeage par nanocavités sur les techniques traditionnelles a toutefois été démontrée pour de nombreuses impuretés métalliques telles le cuivre, le nickel, l'or et le fer. L'efficacité des nanocavités est due au fort lien covalent qui se forme entre l'atome de métal piégé et les liens brisés de silicium situés sur les parois des cavités.

L'utilisation potentielle de cette nouvelle technique de piégeage a grandement stimulé la recherche dans le domaine des nanocavités. Des implantations d'hélium à basse énergie sont généralement utilisées pour créer les systèmes de cavités bien que Williams et al.[3] aient montré plus récemment qu'une implantation d'hydrogène à haute dose permet d'obtenir un résultat équivalent. Quoiqu'il en soit, la fabrication de dispositifs à intégration à très grande échelle (VLSI) requiert non seulement de faibles concentrations d'impuretés métalliques mais également une faible densité de défauts. Ainsi, du point de vue de l'optimisation du procédé de fabrication, il serait désirable de réduire les doses nécessaires à la création des nanocavités.

---

[2] *The National Technology Roadmap for Semiconductors* (Semiconductor Industry Assoc., San Jose, CA, 1997).

[3] J. Wong-Leung, J.S. Williams, R.G. Elliman, E. Nygren, D.J. Eaglesham, D.C. Jacobson, et J.M. Poate, Nucl. Instrum. Methods B **96**, 253 (1995).

De plus, pour que cette technique soit adoptée par l'industrie des semi-conducteurs, il est nécessaire de pouvoir contrôler la profondeur à laquelle les nanocavités sont formées, leur taille moyenne ainsi que leur stabilité lors de traitements thermiques subséquents. Bien que de nombreux articles soient consacrées à ces sujets, les interactions microscopiques à l'origine de la formation de nanobulles sont encore peu étudiées.

Les nanocavités obtenues après implantation d'hélium sont en fait le résultat final de plusieurs phénomènes incluant la précipitation de l'hélium sous forme de bulles dans la région défectueuse créée durant l'implantation, la croissance des nanobulles sous l'effet de la pression interne et finalement le dépiégeage progressif des atomes d'hélium qui diffusent vers l'extérieur de l'échantillon. Le processus d'agglomération de l'hélium dans le silicium lors de la première phase de la formation de cavités est cependant encore peu compris, tout comme l'importance des défauts lors de la précipitation de l'hélium en nanobulles.

Dans ce travail, nous nous intéressons dans un premier temps aux nanocavités en tant que sites de piégeage d'impuretés d'or. Nous voulons déterminer quantitativement l'influence de la taille des cavités sur leur efficacité de piégeage. Pour ce faire, nous observons le transport et le piégeage d'atomes d'or entre deux couches de nanocavités de différentes dimensions. Nous proposons des effets de courbure et de reconstruction de surface pour expliquer les résultats obtenus.

Dans la seconde partie, nous étudions le processus de nucléation de nanobulles dans le silicium. Pour ce faire, nous recherchons les doses critiques

nécessaires à la formation de cavités en utilisant des implantations d'hydrogène et d'hélium. Les effets chimique de l'hydrogène (passivation des liens brisés de silicium) et physique de l'hélium (source de pression interne) sont combinés de façon à pouvoir diminuer les doses totales requises. Un modèle simple de nucléation de nanobulles basé sur la diminution de l'énergie libre de surface par la présence de l'hydrogène est également présenté.

I. INFLUENCE OF CURVATURE ON IMPURITY GETTERING BY NANOCAVITIES IN Si

Auteurs : François Schiettekatte, Carl Wintgens et Sjoerd Roorda

Influence of curvature on impurity gettering by nanocavities in Si

François Schiettekatte, Carl Wintgens, and Sjoerd Roorda

Groupe de recherche en science et technologie des couches minces et Département de physique, Université de Montréal, ███████████████

ABSTRACT

Competition for Au gettering in Si between two cavity layers of different diameter (34 nm and 12 nm) is examined. Au is initially contained in the large cavity layer made by He implantation. Transport of Au towards the second, small diameter cavity layer is measured by ion scattering. The true surface in both layers is determined by electron microscopy. Small cavities are found to be four times more efficient gettering sites than large cavities for the same amount of internal surface. This difference is explained by a simple model based on curvature thermodynamics, faceting, and surface reconstruction.

Metallic impurities are notorious for their detrimental effect on silicon-based devices.[1] Proximity gettering to hydrogen or helium induced cavities has been found to be an efficient method to control the impurity concentration in the active area of these devices,[2,3] especially for monovalent atoms such as Cu, Ag, Pt, and Au. Recently, Myers *et al.* determined ΔG, the binding free energy, for several transition metal contaminations in silicon[4,5] trapped at such cavities. For Au, this energy was deduced from the detrapping kinetics and found to be near 2.4 eV. Nanocavities act as gettering sites, probably because they contain a pure, unoxidized, and almost uncontaminated surface, but that in itself does not explain the large value of ΔG found by Myers *et al.* The binding energy was also found to decrease with increasing cavity formation temperature. The authors suggested that this effect resulted from the entropy term in the binding free energy or from changes in the chemisorption states with temperature.

We propose that the strong curvature of the nanocavities contributes to its gettering efficiency. The curvature of a surface changes the surface energy due to capillary and surface tension effects.[6] Especially, it influences the chemical potential μ of adsorbed atoms proportionally to the surface curvature. Given [*i*] the atomic fraction of interstitial impurities present in a bulk material in equilibrium with impurities bound to the surface of cavities for which θ is the average fraction of occupied sites. In the case of a weakly contaminated cavity ($\theta \ll 1$), the chemical potential of this system can be expressed as

$$\mu_0 + kT \ln[i] = kT \ln\left[\frac{\theta}{1-\theta}\right] - \beta, \quad \beta = \frac{2\gamma}{R}\frac{V^{\text{mol}}}{N_A}. \tag{1}$$

The first term on right hand side is the Langmuir isotherm[6] for a flat surface. β is the curvature contribution to the chemical potential for which γ is the surface tension of a cavity while R is its radius. V^{mol} is the molar volume of the bulk material and N_A the Avogadro's number. Thus, it appears that a layer formed on a curved surface will be energetically favorable. Moreover, the $1/R$ dependency should make smaller cavities more efficient than larger ones.

In order to verify if this assumption holds for metallic impurities adsorbed on a cavity surface, we measured the impurity transport and equilibrium between two layers with cavities of different diameters. Cavities are usually formed by implanting He or H followed by annealing. Their size, and consequently the curvature of their surface, is mainly determined by the annealing temperature after H or He implantation, as shown by early experiments.[7]

Samples used in this study were <100> Czochralski (Cz) silicon wafers (n-type, 10-15 Ωcm, 500 μm thick). He ions were first implanted into the samples with a dose of 1×10^{17} cm^{-2} at an energy of 100 keV at room temperature. Wafers were then annealed in vacuum at 1273 K for 1 h in order to form a layer of large nanometer-size cavities. The samples were further implanted with Au ions to a dose of 1×10^{14} cm^{-2}, followed by annealing at 1173 K for 3 h to induce gettering of the implanted impurities to the first cavity layer. A second layer of smaller cavities was obtained by implanting 30 keV He ions to a dose of 3×10^{16} cm^{-2}.

Finally, a series of isothermal anneals was performed at 1073 K in order to form the second layer of nanocavities and to observe the redistribution of Au between layers.

The density and size of nanocavities in each layer were determined by cross-sectional transmission electron microscopy (XTEM) carried out in bright field mode on a Philips CM-30 microscope operating at 300 kV. A micrograph with both cavity layers is shown in Fig. 1. As reported under *interlayer data* in Table I, the cavities in the first layer, formed at 1273 K, have a mean diameter $\varnothing_1$ of 31 nm. The distribution follows the implanted He depth profile, which has a mean range of 700 nm. The mean diameter $\varnothing_2$ of the cavities in the second layer is 12 nm. This layer was formed during the 1073 K annealing. It is known that within 15 minutes at 1073 K, the cavity size stabilizes at this value.[7] The ratio of true surface amount in layer 2 over layer 1 (A_2/A_1) is also calculated. However, a more careful examination of Fig. 1 reveals that the back end of layer 1 is populated with a significant amount of small cavities. Their size is comparable to those in layer 2 and their number is about 1/3 of the total number of cavities in layer 2. The remaining large cavities in layer 1 have an average diameter of 34 nm. The ratio A_2/A_1, which now designates the surface ratio of small to large cavities, is also increased as shown in Table I under *small vs large cavities*.

In order to establish the relative gettering efficiency of the two cavity layers, the impurity transport process between them was examined. Depth profiles of redistributed Au were measured by Rutherford backscattering spectrometry (RBS) employing 2 MeV He ions scattered through 170°. The sample holder was tilted 5°

off the incident beam to avoid channelling. The time progression of the Au concentration in both cavity layers during the second annealing is illustrated in Fig. 2. A Au peak progressively appears in the region of layer 2. After 1 h of annealing only a relatively small amount of Au reached the layer 2. Also, it appears that Au in layer 1 decreases asymmetrically. In fact, the Au concentration in the back end of layer 1 remains almost constant. Because the Au profiles were both measured at equilibrium (before and after introduction of the second cavity layer) it follows immediately that the binding energy is larger in the smaller cavities (backside of the peak) than in the larger cavities (front side of the peak).

The Au concentration in each layer and at the surface is plotted in Fig. 3 against the duration of the second annealing. While the surface Au concentration is constant and negligible, the total concentration decreases with time. This is due to the fact that the Au interstitials are progressively lost to the bulk until their concentration throughout the sample depth is in equilibrium with the gettering sites. From Fig. 3, the amount of "lost" Au at equilibrium is 2.1×10^{13} Au/cm^2. Divided by the sample thickness (0.05 cm), this gives 4.2×10^{14} Au/cm^3, which corresponds to the substitutional Au solubility at 1073 K.[1] It is also seen in Fig. 3 that it takes several hours before appreciable Au is trapped at the small cavity layer. Because this is more than the 15 min. required for cavity formation, these two processes can be treated as independent.

After long-term equilibrium has been reached, the ratio of Au trapped in both cavity layers is $Q_2/Q_1 = 0.40$ whereas the ratio of surface area is only $A_2/A_1 = 0.13$. We thus find that for an equivalent amount of cavity surface, the cavities in

layer 2 are three times more efficient than those of layer 1. Knowing that the smaller cavities are more efficient gettering sites than the larger cavities, we now attribute the asymmetry in the RBS signal to the uneven size distribution of cavities in layer 1. Apparently, only the Au from the large cavities situated between 500 and 700 nm (about 5/6 of the Au) is redistributed, and this has been taken into account in the second column of Table I, labeled *"small vs large cavities."* This result demonstrates that small 12 nm cavities are in fact 4.1 times more efficient than large 34 nm cavities for the same amount of cavity surface.

Concerning the transient part of Fig. 3, the present experiment can be treated as two thin cavity layers separated by the distance Δx and exchanging interstitial impurities in a steady-state diffusion process.[5] All the Q_T impurities are contained in layer 1 at time $t = 0$. Through Eq. (1), and for small contamination ($\theta \ll 1$), it can be shown that the Au concentration Q_n in each layer is expressed by

$$Q_1(t,T) = Q_T - Q_2(t,T) = Q_T[(1-\alpha)e^{-t/\tau} + \alpha], \tag{2}$$

where α is the fraction of impurities remaining in layer 1 at equilibrium ($t \gg \tau$) and

$$\tau = \left[\frac{\alpha S_2}{e^{-(\mu_0 + \beta_2)/kT}} \frac{\Delta x}{N_{Si} D_{imp}} \right]. \tag{3}$$

Here, N_{Si} is the atom density of silicon and D_{imp} the diffusion coefficient of the impurities in their interstitial state. S_2 is the areal density of sites in layer 2 ($\theta_n =$

Q_n/S_n). Consequently, $\mu_0+\beta_2$, the effective chemical potential for cavity layer 2, can be deduced from τ, provided that the other parameters of Eq. (3) are known.

A least-squares fit of Eq. (2) was applied to the Au concentration evolution in both cavity layers and appears as solid lines in Fig. 3. These equations were weighted by a function of the form $(1-\lambda_1)\exp(-\lambda_2 t) + \lambda_1$ to take into account the "lost" Au dissolved into the bulk. The parameters returned by this fit are shown in Table I. With an interstitial Au diffusivity[1] of $D_{imp} = 3.5\times10^{-6}$ cm^2/s, assuming $S_2 = 1.5\times10^{14}$ cm^{-2}, and with $\Delta x = 400$ nm, we find from Eq. (3) that $\mu_0+\beta_2 = 2.5\pm0.1$ eV. This is close to the above-mentioned value of ΔG in Ref. 5. The uncertainty in $\mu_0+\beta_2$ is mainly due to the uncertainty in S_2 and D_{imp}.

Let us now evaluate if the difference in gettering efficiency is indeed a consequence of capillary effects. First, a value for β can be predicted [Eq. (1)]. Given $a = 0.543$ nm the Si lattice parameter, $V^{mol}/N_A = a^3/8$. For a solid surface where an areal density n of bonds of energy ϕ are broken, $\gamma = fn\phi/2$ where f is a geometrical factor between 1 and $\sqrt{3}$ for vicinal surfaces.[6] The density of dangling bonds $n = 4/a^2\sqrt{3}$ for an unreconstructed <111> surface and $\sqrt{3}$ larger for an unreconstructed <100> surface. From these definitions we find,

$$\beta = \phi \frac{f}{2\sqrt{3}} \frac{a}{R}. \tag{4}$$

The cavities of layer 1 appear faceted in the <111> direction, therefore we assume $f_1 \approx 1$. With $\phi = 1.8$ eV for Si-Si bonds, we find $\beta_1 = 17$ meV. For layer 2, the

mean value of f_2 falls between 1 and $\sqrt{3}$ depending on the orientation. Consequently, β_2 ranges from 44 meV to 76 meV. The effect of curvature on the binding energy would amount to $\beta_2 - \beta_1 = 27$-59 meV.

Based on the measured Au distribution at equilibrium (Q_1/Q_2) and for small Au coverage ($\theta \ll 1$), we can determine $\beta_2 - \beta_1$ according to the difference in chemical potential [Eq. (1)]:

$$\beta_2 - \beta_1 = kT \ln\left[\frac{\theta_2}{\theta_1}\right] = kT \ln\left[\frac{(1-\alpha)}{\alpha}\frac{k_1 A_1}{k_2 A_2}\right], \tag{5}$$

where the subscripts denote the values for each layer. While f_n already accounts for the geometrical effects on the areal density of gettering sites, k_n will do so for surface reconstruction effects, since $S_n = k_n A_n$. Assuming that the density of sites is the same within all cavities ($k_1/k_2 = 1$) we find from Eq. (5) that $\beta_2 - \beta_1 = 130$ meV which is 2-4 times higher than the calculated value of $\beta_2 - \beta_1$. It appears that surface reconstruction effects do play a role, and $k_1/k_2 < 1$.

The 7×7 and Au-induced 5×2 reconstruction of <111> orientation have been widely studied on the external surface of silicon.[8] For Au coverage less than 1/2 monolayer, 7×7 Au-free domains (formed above 700 K) coexist with 5×2 domains. Each 5×2 cell can accommodate seven Au atoms, instead of ten for equivalent 1×1 surface. Thus, if the large cavity surfaces were fully reconstructed, at least 35% of the bonds remain available. This is a lower limit since large cavities also contain unreconstructed curved surfaces. Moreover, it is not excluded

that some reconstruction in small cavities occurs. The measured Au redistribution and the estimates of β_2-β_1, from curvature arguments, imply k_1/k_2 values from 33% to 47%. We thus conclude that curvature thermodynamic and surface reconstruction effects both contribute to efficient gettering in nanocavities.

In summary, experimental measurements of the Au transport between two cavity layers show that small 12 nm cavities are more efficient than large 34 nm cavities by a factor of 4.1 for equivalent amount of surface. The measured difference in *effective* trapping energy is 0.13 eV in this case. This is explained in part by the possibility of surface reconstruction in large cavities, which reduces the number of available dangling bonds, and by the effect of curvature and surface tension on the chemical potential in cavities.

[1] K. Graff, *Metal Impurities in Silicon-device Fabrication* (Springer, Berlin, 1995).

[2] S. M. Myers, D. M. Bishop, D. M. Follstaedt, H. J. Stein, and W. R. Wampler, Mater. Res. Soc. Symp. Proc. **283**, 549 (1993).

[3] J. Wong-Leung, C. E. Ascheron, M. Petravic, R. G. Elliman, and J. S. Williams, Appl. Phys. Lett. **66**, 1231 (1995).

[4] S. M. Myers, G. A. Petersen, and C. H. Seager, J. Appl. Phys. **80**, 3717 (1996).

[5] S. M. Myers and G. A. Petersen, Phys. Rev. B **57**, 7015 (1998).

[6] J. B. Hudson, *Surface Science: An Introduction* (Butterworth-Heinemann, Boston, 1991).

[7] V. Raineri, A. Battaglia, and E. Rimini, Nucl. Instrum. Methods Phys. Res. B **96**, 249 (1995).

[8] J. D. O'Mahony, J. F. McGilp, C. F. J. Flipse, P. Weightman, and F. M. Leibsle, Phys. Rev. B **49**, 2527 (1994).

Table Caption

Table I. Diameters ($\varnothing$) and area ratio extracted from Fig. 1; ratio of Au

concentration Q_i in each layer at equilibrium from Fig. 3 and relative

efficiency of layer 2 over layer 1 per unit area of cavity surface; fitting

parameters of Eq. (2) to Fig. 3; resulting $\beta_2 - \beta_1$.

	Interlayer data	Small vs large cavities
$\varnothing_1$ [nm]	31 ± 15[a]	34 ± 13[a]
$\varnothing_2$ [nm]	12 ± 5[a]	12 ± 5[a]
A_2/A_1	0.13 ± 0.01	0.16
Q_2/Q_1 at $t\rightarrow\infty$	0.40 ± 0.01	0.65
Efficiency	3.1	4.1
Q_T [Au/nm^2]	1.06	1.06
α	0.72 ± 0.01	0.6
τ [h]	1.8 ± 0.1	...
$\beta_2 - \beta_1$ calculated		43 ± 16 meV
$\beta_2 - \beta_1$ for $S_2/S_1 \approx A_2/A_1$		130 meV
k_1/k_2 for calculated $\beta_2 - \beta_1$		$40\pm7\%$

[a]Standard deviation over cavity population.

Table I

Figure Captions

Fig. 1.   XTEM micrograph of a sample with two cavity layers. (1) first layer,

(2) second layer, (s) surface.

Fig. 2.   Au depth profile evolution with time during annealing of second cavity

layer at 1073 K; after 0 (— — —), 1 (- - -) and 30 h (——).

Fig. 3.   Evolution of Au concentration in layer 1 (□), layer 2 (◇) and at surface

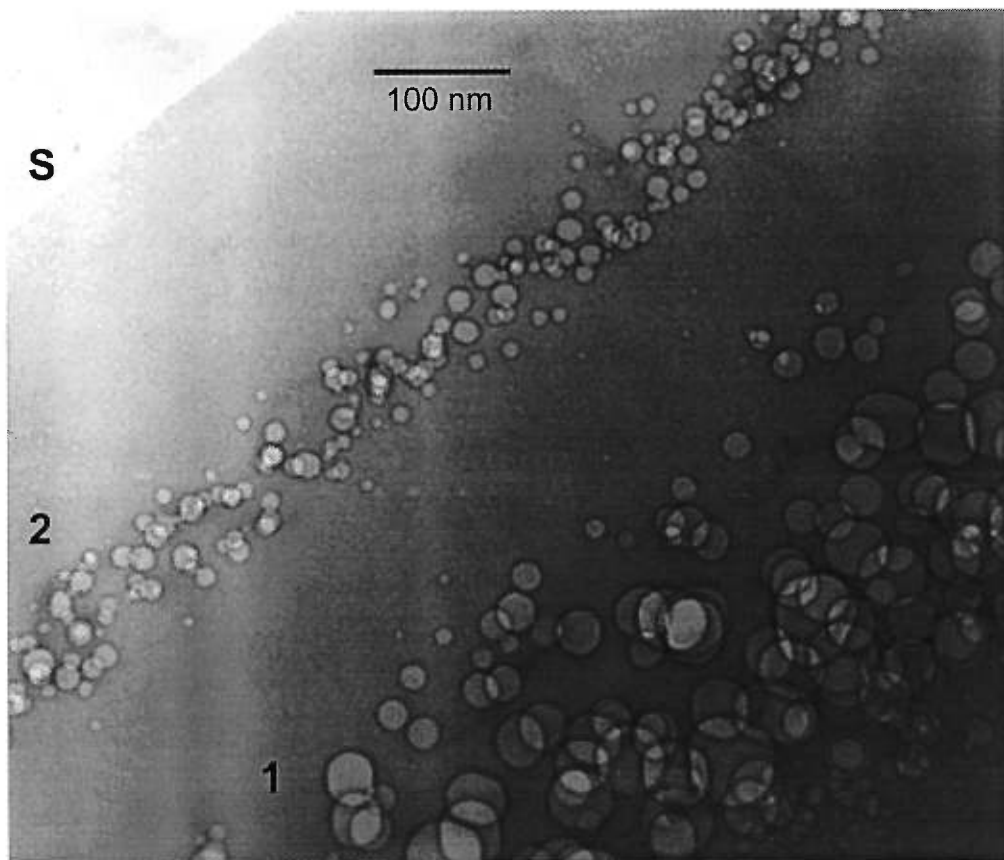(- - -) during second annealing (at 1073 K). Total concentration also

appears (○).

Figure 1

Figure 2

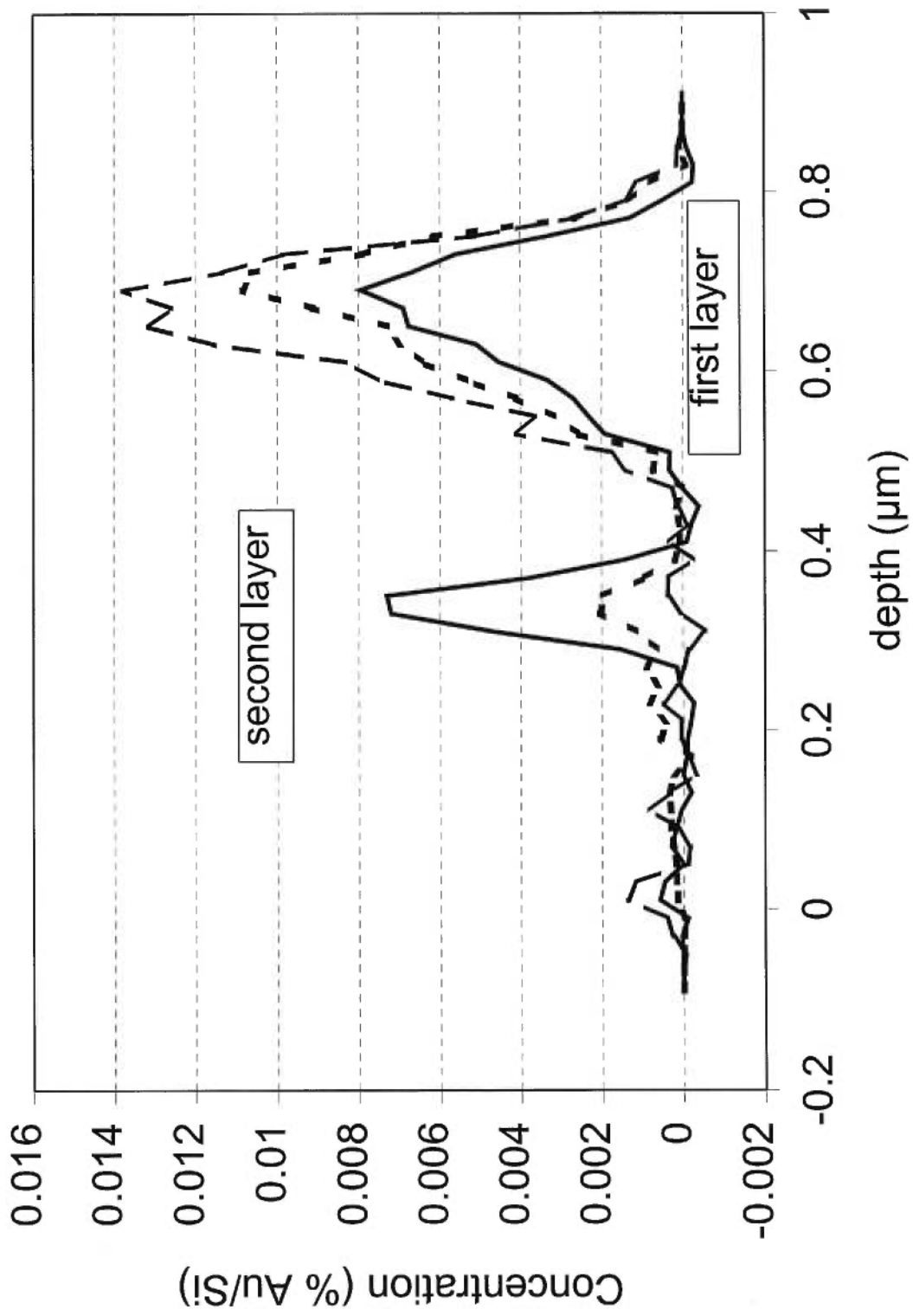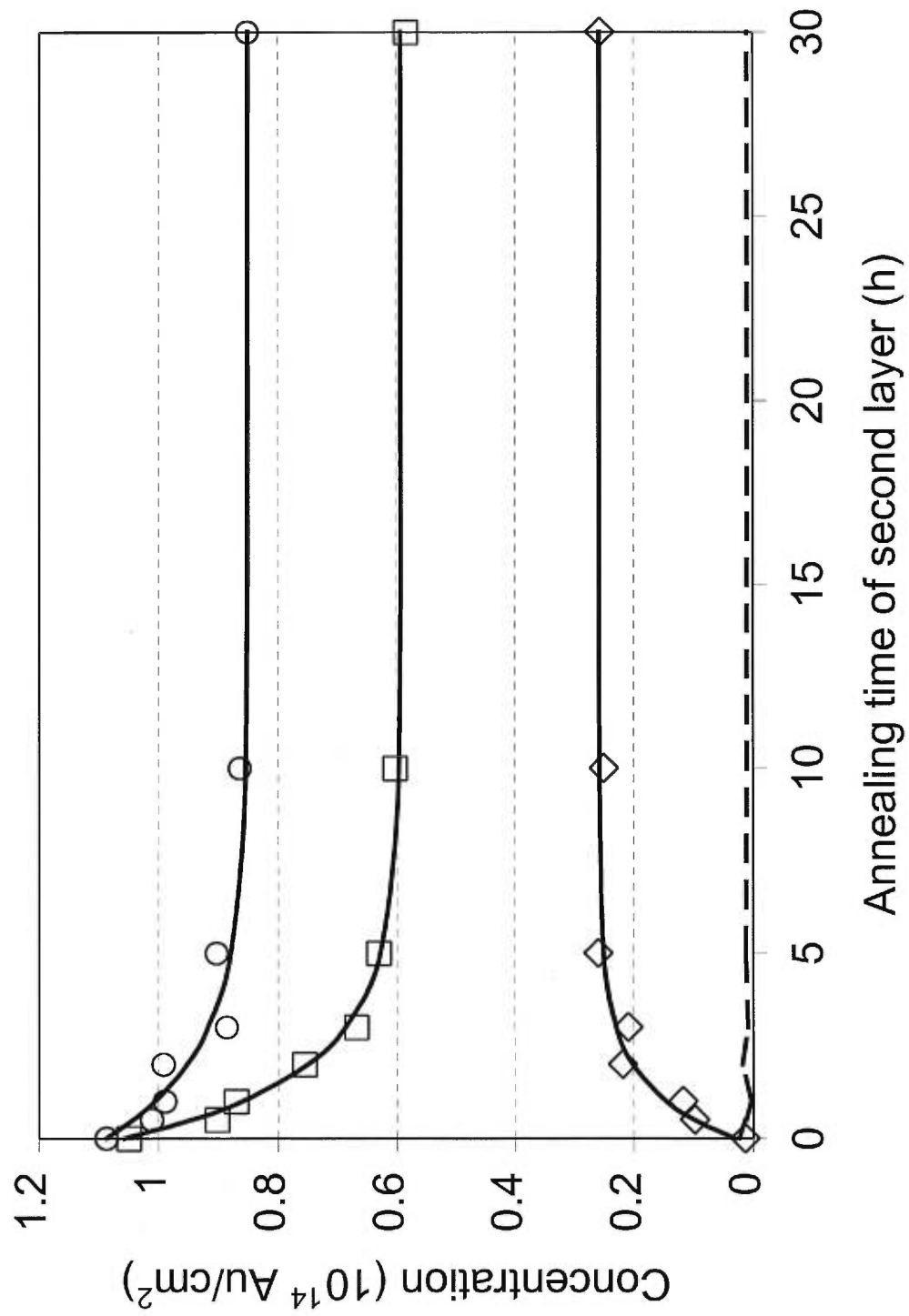Figure 3

II. EFFICIENT NUCLEATION OF NANOCAVITIES IN Si BY H/He CO-IMPLANTATION

Auteurs : Carl Wintgens, François Schiettekatte, Sjoerd Roorda

et Peter J. Simpson

Efficient nucleation of nanocavities in Si by H/He co-implantation

Carl Wintgens, François Schiettekatte, and Sjoerd Roorda

Groupe de recherche en science et technologie des couches minces et Département de physique, Université de Montréal, █████████████████████

Peter J. Simpson

Department of Physics and Astronomy, The University of Western Ontario, ███████
████████████

ABSTRACT

We investigate the critical dose necessary for nanocavity formation in silicon via H/He co-implantation. The presence of cavities is deduced from the transport and gettering of intentionally introduced Au, monitored by Rutherford backscattering spectrometry. Positron annihilation spectroscopy is used to confirm the presence of voids in Si. We find that the combined effect of H/He can reduce the total critical dose by 36% and 63% compared to He-only and H-only implantations, respectively. A physical model which yields good agreement with these results is presented, in which the enhanced efficiency of co-implantation is due to a reduction in surface tension at the cavity surface as a result of the passivation of Si dangling bonds by hydrogen.

There has recently been a renewed interest in the nanometer-size voids created after high temperature annealing of hydrogen-implanted or helium-implanted silicon. The ability of these cavities to getter metallic impurities has been demonstrated on several occasions and for different transition metals, particularly Cu, Pt and Au which are known to degrade the performance of microelectronic devices.[1-5] Despite its proven efficiency, this gettering technique has some drawbacks which deter its use for Si device processing, such as the relatively high implantation doses required ($>10^{16}$ cm^{-2}).

Two approaches to obtain nanocavities in silicon for gettering purposes have been explored : He ion implantation[6] and H implantation.[7] Even though hydrogen and helium are both light gases, they behave very differently in silicon. H ions interact chemically with silicon, passivating unreconstructed Si dangling bonds created during implantation and thus lowering the energy of internal surfaces. He ions are thought to have a more mechanical role by providing the pressure that drives the growth of the cavities. Since nanocavity formation involves both the creation of an internal surface and a force-driven expansion,[8] it might then be expected that co-implantation of H and He would be more effective than the implantation of a single element.

The idea of combining the different effects of hydrogen and helium was initially proposed to improve the thin film separation technique for silicon-on-insulator (SOI) film fabrication by the "Smart Cut" method.[9] In this article, we use H/He co-implantation to increase efficiently the nanocavity nucleation in silicon and to lower the required total dose compared to pure H or He implantations. We

also propose a quantitative model based on surface tension effects to explain the results.

The samples used in this experiment were (100) Czochralski Si wafers (n-type, 10-15 Ωcm, 500 μm thick). H$^-$ ions were first implanted at room temperature with an energy of 45 keV. He$^+$ ions were then implanted at 50 keV so that the distribution essentially overlaps the H depth profile (projected range R_p of 495 nm according to SRIM2000 Monte-Carlo simulations).[10] The total doses ranged from 1×10^{15} to 4×10^{16} cm^{-2}. The samples were annealed in vacuum at 1173 K for 1 h in order to form and enlarge the cavities and to activate the out-diffusion of the implanted gases from the specimens. Some of the samples were further implanted with 1×10^{14} cm^{-2} Au ions at 300 keV (1/5 of the H/He projected range). These specimens were again annealed at 1173 K for 1 h to induce gettering of the implanted Au at available trapping sites. Depth profiles of redistributed Au were then monitored by Rutherford Backscattering Spectrometry (RBS) using 2 MeV He ions scattered through 170°.

In addition, some samples not implanted with Au were analyzed by Positron Annihilation Spectroscopy (PAS) in order to obtain the distribution of open-volume defects. Doppler-broadening of the positron annihilation line was measured using a high-purity Ge detector. The shape of the 511 keV annihilation line was characterized by the S parameter defined as the ratio of the counts in the central area of the peak ($|511-E_\gamma| \leq 0.7$ keV) to the total area of the peak ($|511-E_\gamma| \leq 6.6$ keV). Open volume defects in the sample cause a narrowing of the annihilation line due to reduced interaction of positrons with fast-moving core

electrons, and so increase the value of *S*. Probing depth is controlled by scanning the e^+ implantation energy range from 0.5 to 50 keV, corresponding to a mean depth from ~5 nm to ~11 μm in Si.

Since the nanocavities act as strong gettering sites for metallic impurities, the first approach to detect the presence of cavities was to measure the quantity of Au trapped at the H/He mean depth range after annealing. If more than 80% of the total implanted Au is gettered at the expected cavities depth, it is concluded that voids are probably formed. If there is no cavity nucleation, the Au will be adsorbed at the sample surface or will precipitate at extended defects created for less-than-critical doses, both representing considerably less efficient gettering sites. In all cases, a small fraction of gold is dissolved as immobile, substitutional Au and becomes essentially lost in the bulk of the sample.[4]

Fig. 1 illustrates the redistribution of Au after annealing as monitored by RBS for two samples previously co-implanted with 60% H and 40% He to a total dose of 1×10^{16} cm^{-2} and 5×10^{15} cm^{-2}, respectively above and below the critical dose for cavity nucleation. For a combined (H+He) dose of 1×10^{16} cm^{-2}, more than 90% of the Au has moved from the as-implanted region to the H/He depth (~500 nm) as illustrated by the solid line. Considering the high gettering efficiency, it is likely that Au atoms are chemisorbed at the surface of the cavities created by the H/He implantation. However, the presence of such cavities needs to be confirmed, which will be discussed below. In the case of a total dose of 5×10^{15} cm^{-2}, with the same H/He proportion, most of the Au atoms are trapped at the surface.

Consequently, this dose must be below the minimum required for cavity formation.

Implantation to several total doses and for different hydrogen fractions (H dose/total dose) have been carried out in order to determine the threshold region for nanocavity nucleation. Only the results near the threshold have been reported in Fig. 2. The minimum total dose for cavity formation is included between an "×" and a "•" symbol representing respectively the absence and the presence of cavities at this particular hydrogen fraction as determined by the gettering of Au.

We find a critical dose for He-only implantation near 1×10^{16} cm^{-2} which is consistent with the results found in earlier work.[11,12] It is seen in Fig. 2 that the critical dose for He-only implantation is 42% smaller than that for H only. But the most important feature of this figure is that a 50/50 proportion of the two elements further allows a 36% reduction of the total critical dose compared to He-only implantation. This result demonstrates the synergistic effect of H/He co-implantation in the formation of nanocavities.

The results of Fig. 3 clarify the roles of hydrogen and helium in the cavity nucleation process. It demonstrates that their effect is not simply additive and that a more complex interplay exists between the two species. For this sample, helium was implanted at an energy of 50 keV, as for the other samples, and to a dose of 1.6×10^{16} cm^{-2}. But this time, hydrogen was implanted at only 23 keV (R_p=300 nm instead of 450 nm) and to a sub-critical dose of 8×10^{15} cm^{-2}. It is seen that the cavities are formed at the H implantation depth, which strongly suggests that helium diffuses to the hydrogen region instead of nucleating cavities at its own

mean depth range. The behavior of H is consequently consistent with the one of a chemically active species, readily passivating dangling silicon bonds created during implantation. The migration of He is explained by the fact that it is not easily trapped at broken silicon bonds. Because it has an extremely low solubility in silicon, it tends to segregate to the microvoids created by H implantation.

As we mentioned before, Au gettering is only an indirect evidence for the presence of cavities. In order to confirm that cavities do exist for near-critical co-implantation doses, PAS was used to obtain the depth profile of open volume defects for ion doses just above the critical region for nanocavity nucleation. The detection of voids by TEM measurements turned out to be difficult due to the small cavity size and low densities produced with doses lower than 10^{16} cm^{-2}. PAS has been shown[13,14] to be highly sensitive to vacancy-like defects and particularly small cavities because of the tendency of positrons to annihilate at sites where the atomic core repulsion is minimum. For the sake of clarity, the difference of the S parameter of the samples to the corresponding value of a reference sample has been plotted.[15] In this case, the reference sample was implanted with 5×10^{15} He/cm^2, a dose below the critical region for He-only implantation. Fig. 4 shows the ΔS values as a function of positron implantation energy for samples implanted to a total dose of 1×10^{16} cm^{-2}, with H fractions of 40%, 50% and 60%. Also, the results for H-only and He-only implantations at the higher typical dose of 3×10^{16} cm^{-2} are presented for comparison. It is important to note that the implanted gases are evacuated from the samples during the 900°C annealing and that the amount of bound (Si-H) hydrogen is negligible at this temperature as shown by IR

spectroscopy measurements.[16]

According to Fig. 4, in the 8-12 keV energy range (corresponding to a mean depth of 500 - 1000 nm), the S values of the samples are higher than those of the reference sample. This difference indicates that an increased fraction of positrons annihilates with low-momentum electrons and is a characteristic of positron trapped at open volume defects. Fig. 4 shows a maximum number of open volume defects (or cavities) for a H fraction of 50%. We can therefore conclude that the minimum critical dose for nanocavity formation is reached for a 50/50 proportion of H and He. Also, for the same relatively high implantation dose of 3×10^{16} cm^{-2}, we see that H is less efficient at producing nanocavities than He.

In the next section, we propose a model in order to explain the synergistic effect of H/He co-implantation. First, the process of nanocavity formation by He-only implantation in Si can be summarized in 3 major steps:

1. Because of its extremely low solubility, as-implanted helium precipitates into small bubbles (the precursors of the cavities) at the defect layer produced by the implantation.

2. Upon annealing, the cavities grow and coalesce in a well defined layer because of the high pressure of helium inside the cavities.

3. Helium is progressively detrapped from the bubbles and diffuses out of the sample, leaving stable nanometer-size cavities.

Here, we propose a model of precursor bubble nucleation in Si that will take into account a decrease of the surface tension due to the presence of hydrogen. The model estimates the critical quantity of H and He necessary for a gas-filled bubble

to be in equilibrium and then possibly grow into a nanocavity. To this end, we will

i.   Assume that all bubbles have the same general size and shape at equilibrium.

ii. Evaluate the surface tension and the corresponding quantity of adsorbed H atoms at the bubble surface.

iii. Estimate the quantity of He atoms and/or H_2 molecules required to satisfy the conditions 1) and 2) according to the model.

It is important to note that the model defines the necessary conditions for cavity precursors to nucleate in Si but doesn't describe the later stages of the growth process (i.e. the formation of stable gas-empty cavities).

Let $\Delta\mu = \mu_{sol} - \mu_{cav}$ be the chemical potential difference between He atoms in solution surrounding a bubble and He atoms inside it. Because of its low solubility in Si, $\Delta\mu$ is positive and thus helium in the bubble will be more stable than in solution. However, the surface tension γ of the gas-filled cavity is positive and tends to increase the free energy of the bubble. The change in Gibbs free energy when a bubble of surface S and volume V forms is given by:

$$\Delta G = G_{cav} - G_{sol} = -n_{He}V\Delta\mu + S\gamma, \qquad (1)$$

where n_{He} is the density of He atoms in the bubble. An approximate value of $\Delta\mu$ can be obtained from thermal desorption measurements,[17] and has been found to lie between 0.3 and 0.45 eV.[18]

At equilibrium, the density of He atoms trapped inside the bubble will be given by Eq. (1) for $\Delta G = 0$. When the concentration of helium is lower than the

equilibrium value, the free energy of the surface will be dominant and the cavity precursor will not be formed. In the case of a He concentration higher than the critical value, the bubble will form and be able to grow by the work of pressure of He inside the cavity when annealed at a sufficiently high temperature (>800°C).

It has been shown that co-implants of hydrogen and helium lead to a buried layer of ellipsoidal bubbles called platelets of typical size 10 nm.[9] We can then start by estimating the equilibrium concentration of He inside an oblate ellipsoid of 10 nm diameter and 1 nm short axis. In this case, the role of hydrogen will be to lower the surface tension of the platelet as described by :

$$\gamma = [\theta_H \phi_{Si-H} + (1 - \theta_H)\phi_{Si}]\nu \tag{2}$$

where ϕ_{Si} is the energy per Si bond[19] and ϕ_{Si-H} is the energy of a Si dangling bond passivated by a H atom.[20] ν is the areal density of broken bonds and θ_H is the fraction of dangling bonds passivated by hydrogen.

For the lower fractions of implanted hydrogen, it can safely be assumed that all H atoms will passivate Si dangling bonds created during implantation.[21] The critical dose for cavity nucleation predicted by the model (i.e. at $\Delta G = 0$) for the lower 0-40% H region is illustrated by the solid line plotted against the left vertical axis in Fig. 2. When there is only a small amount of He, the source of internal pressure is demonstrated to be molecular H_2 trapped inside the voids.[16] By extrapolating the data for the domain >40% H (— — — on Fig. 2), we can calculate the fraction of hydrogen in molecular form trapped inside the bubble

compared to adsorbed hydrogen at the cavity surface. This is shown by the dotted line plotted against the right vertical axis in Fig. 2. Also shown on Fig. 2 is θ_H, the theoretical fraction of dangling bonds stabilized by hydrogen obtained from the model.

According to the model, the minimum critical dose for cavity nucleation is attained for the higher coverage of the surface by hydrogen (minimum surface tension). In the 0-40% H region, θ_H is limited by the implanted H doses. On the other hand, for the 60-100% H region, θ_H seems to be limited by the low He doses. In fact, the high fraction of molecular hydrogen when implanting little or no helium may provide a possible explanation for the relative inefficiency of hydrogen to form nanocavities because one needs twice as much H to have the same pressure effect as He. This also tends to confirm the indirect "chemical" role of He, driving the conversion of molecular hydrogen to the bound Si-H state.[16]

In conclusion, we have observed that the threshold dose for nanocavity nucleation in Si is reduced by 36% when co-implanting equal amounts of H and He instead of He only. Also, the formation of cavities is 42% less efficient when using only H compared to He-only implantation. Consequently, the threshold is decreased by a factor of nearly 3 for co-implantation compared to H-only implantation. This enhanced efficiency of H/He co-implantation and the different critical doses for H and He are explained by a simple model in which we take into account the surface tension effects of the nanocavities. These results may be relevant to gettering strategies used in device manufacturing.

[1] V. Raineri, P. G. Fallica, G. Percolla, A. Battaglia, M. Barbagallo, and S. U. Campisano, J. Appl. Phys. **78**, 3727 (1995).

[2] S. M. Myers and G. A. Petersen, Phys. Rev. B **57**, 7015 (1998).

[3] A. Kinomura, J. S. Williams, J. Wong-Leung, and M. Petravic, Appl. Phys. Lett. **72**, 2713 (1998).

[4] F. Schiettekatte, C. Wintgens, and S. Roorda, Appl. Phys. Lett. **74**, 1857 (1999).

[5] K. C. Hall, R. D. Goldberg, T. D. Lowes, P. J. Simpson, I. V. Mitchell, and G. C. Weatherly, Can. J. Phys. (Suppl.) **74**: S248-S251 (1996).

[6] C. C. Griffioen, J. H. Evans, P. C. de Jong, and A. Van Veen, Nucl. Instrum. Methods B **27**, 417 (1987).

[7] J. Wong-Leung, J. S. Williams, R. G. Elliman, E. Nygren, D. J. Eaglesham, D. C. Jacobson, and J. M. Poate, Nucl. Instrum. Methods B **96**, 253 (1995).

[8] W. Fukarek and J. R. Kaschny, J. Appl. Phys. **86**, 4160 (1999).

[9] A. Agarwal, T. E. Haynes, V. C. Venezia, O. W. Holland, and D. J. Eaglesham, Appl. Phys. Lett. **72**, 1086 (1998).

[10] J. F. Ziegler, J. P. Biersack, and U. Littmark, *The Stopping and Range of Ions in Solids* (Pergamon, New York, 1985).

[11] S. M. Myers and D. M. Follstaedt, J. Appl. Phys. **79**, 1337 (1996).

[12] P. F. P. Fichtner, J. R. Kaschny, R. A. Yankov, A. Mücklich, U. Kreissig, and W. Skorupa, Appl. Phys. Lett. **70**, 732 (1997).

[13] P. J. Schultz and K. G. Lynn, Rev. Mod. Phys. **60**, 701 (1988).

[14] D. W. Lawther and P. J. Simpson, Defect and Diffusion Forum **138/139** 1-18

(1996).

[15] R. S. Brusa, G. P. Karwasz, N. Tiengo, A. Zecca, F. Corni, G. Calzolari, and C. Nobili, J. Appl. Phys. **85**, 2390 (1999).

[16] M. K. Weldon, M. Collot, Y. J. Chabal, V. C. Venezia, A. Agarwal, T. E. Haynes, D. J. Eaglesham, S. B. Christman, and E. E. Chaban, Appl. Phys. Lett. **73**, 3721 (1998).

[17] F. Corni, G. Calzolari, S. Frabboni, C. Nobili, G. Ottaviani, R. Tonini, G. F. Cerofolini, D. Leone, M. Servidori, R. S. Brusa, G. P. Karwasz, N. Tiengo, and A. Zecca, J. Appl. Phys. **85**, 1401 (1999).

[18] Although $\Delta\mu$ decreases as the He pressure builds inside the bubble, we consider a constant mean value of $\Delta\mu$ for the simplicity of the model.

[19] T. J. Lenosky, J. D. Kress, I. Kwon, A. F. Voter, B. Edwards, D. F. Richards, S. Yang, and J. B. Adams, Phys. Rev. B **55**, (1997).

[20] M. Cardona, Phys. Stat. Sol. B **118**, 463 (1983).

[21] This is so because He is known to favor the conversion of molecular H_2 to the bound Si-H state, as will be further discussed.

Figure Captions

Fig. 1.   Au depth profiles for sample as-implanted with 1×10^{14} Au/cm^2 (———)

and after annealing at 1173 K for samples previously co-implanted with

40% He and 60% H to a total dose of 5×10^{15} cm-^{2} (- - -) and 1×10^{16} cm-^{2}

(———). The doses are respectively below and above the critical dose for

nanocavity nucleation at this particular hydrogen fraction.

Fig. 2.   Critical region for nanocavity nucleation from H/He co-implantation.

This is established according to the gettering of intentionally introduced

Au. The threshold region is situated above the "×" and below the "•".

Also shown is the critical dose predicted by the model (—, 0-40%H) and

fitted from experimental data (———, 40-100%H). The fraction of

molecular H calculated from the fitted data is illustrated by the - - - curve

(right scale). The theoretical fraction of Si dangling bonds passivated by

H at the cavity surface is represented by the — - - — curve (right scale).

Fig. 3.   Au profiles for samples implanted with H only (———), He only (- - -)

and co-implanted with 33% of H (———). H ions are implanted at half the

energy of He ions. This shows that even for low H fraction, the nano-

cavities are formed near the H mean depth range.

Fig. 4. ΔS vs positron implantation energy for samples implanted with He only and H only at a fluence of 3×10^{16} cm^{-2} and also to a total dose of 1×10^{16} cm^{-2} for 40, 50 and 60% H fractions. Reference sample implanted at a 5×10^{15} cm^{-2} fluence of He. All samples annealed at 1173 K for 1h.
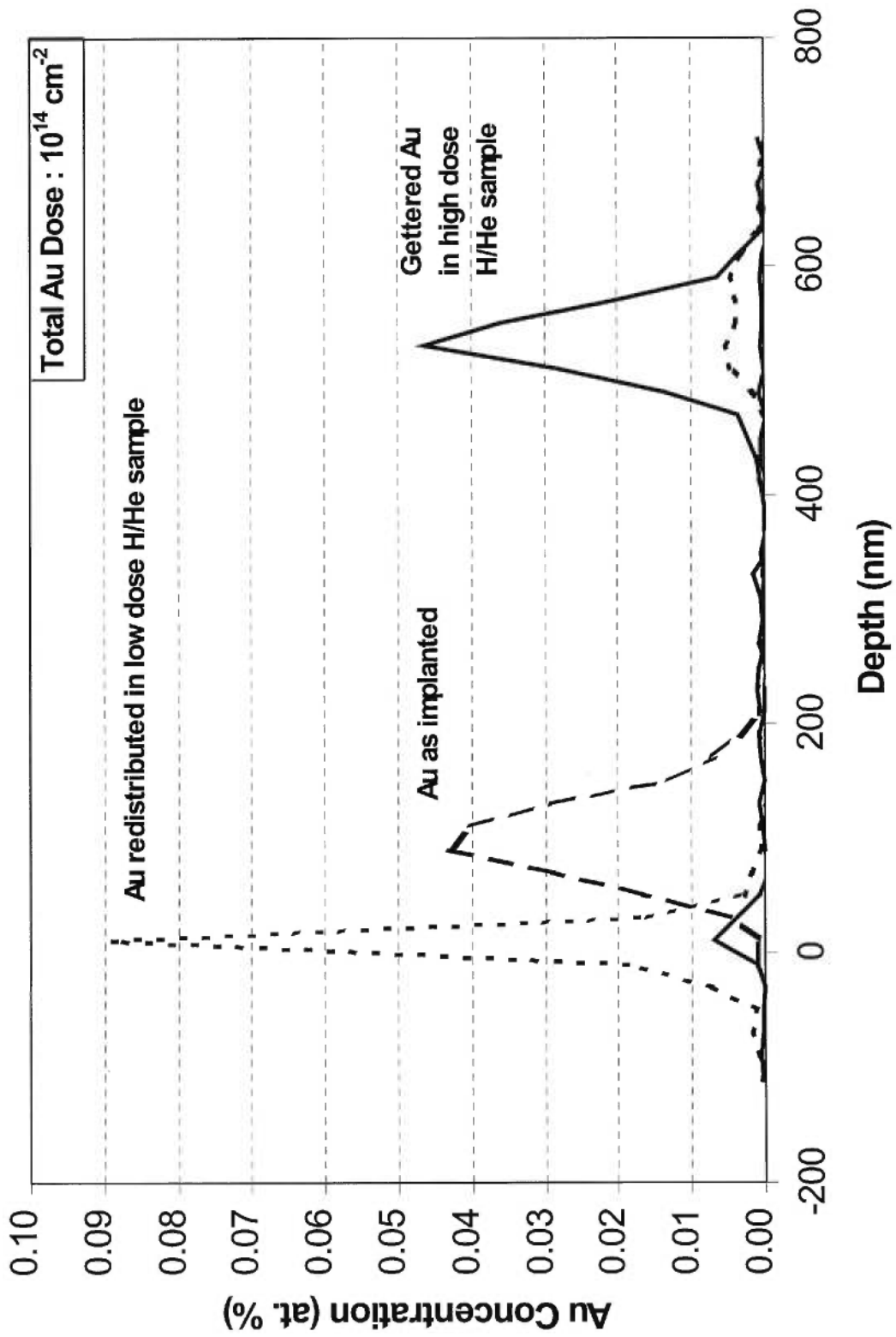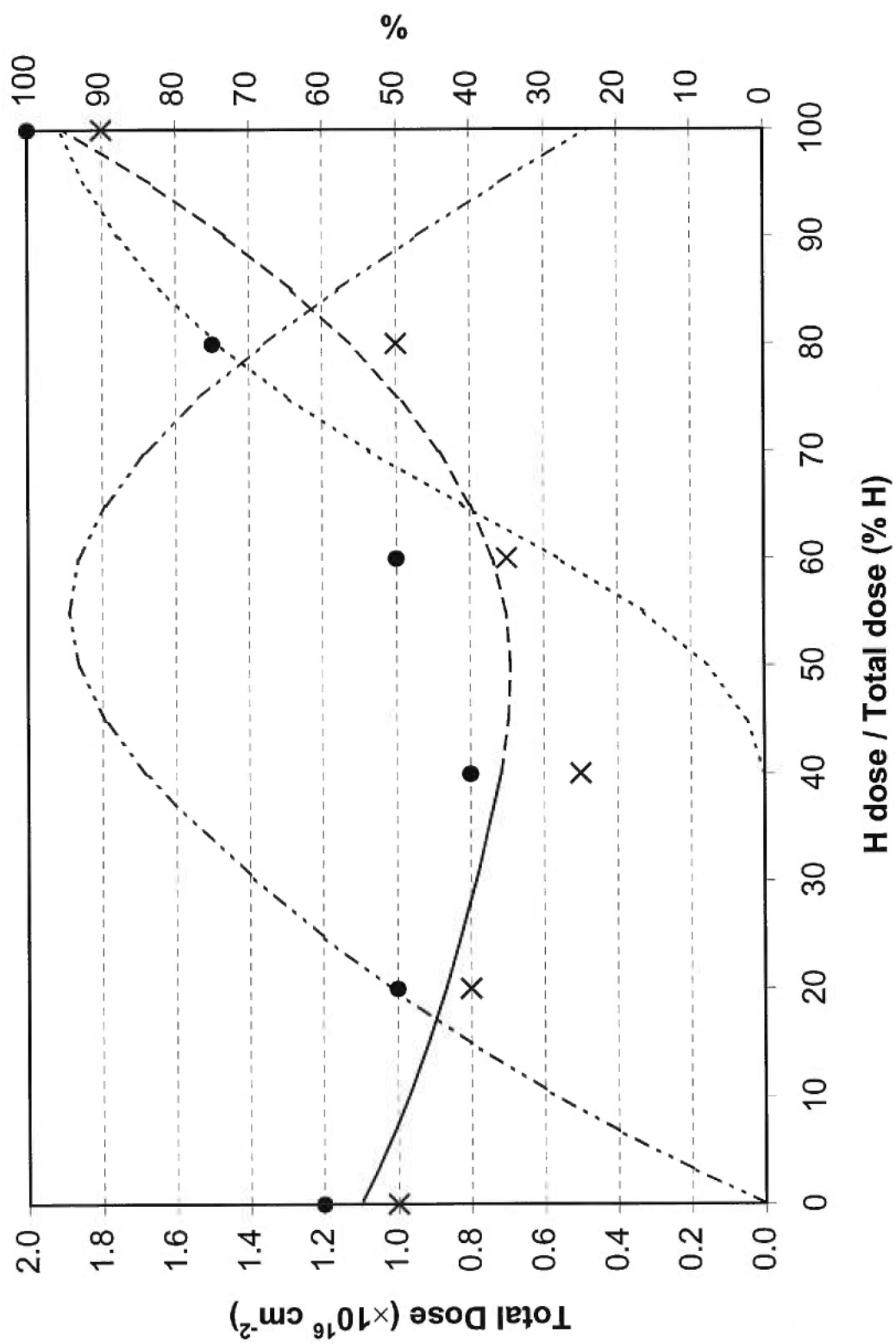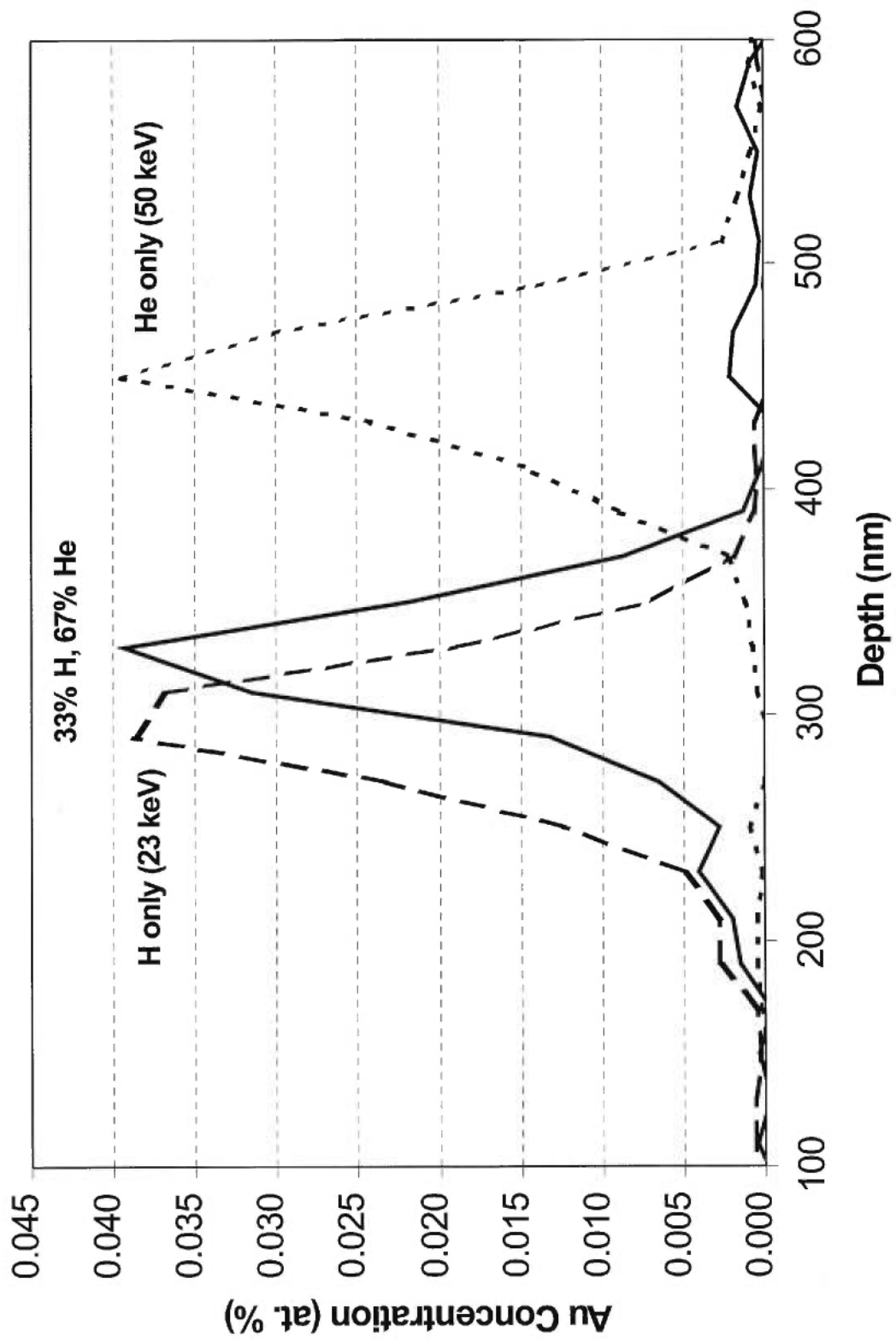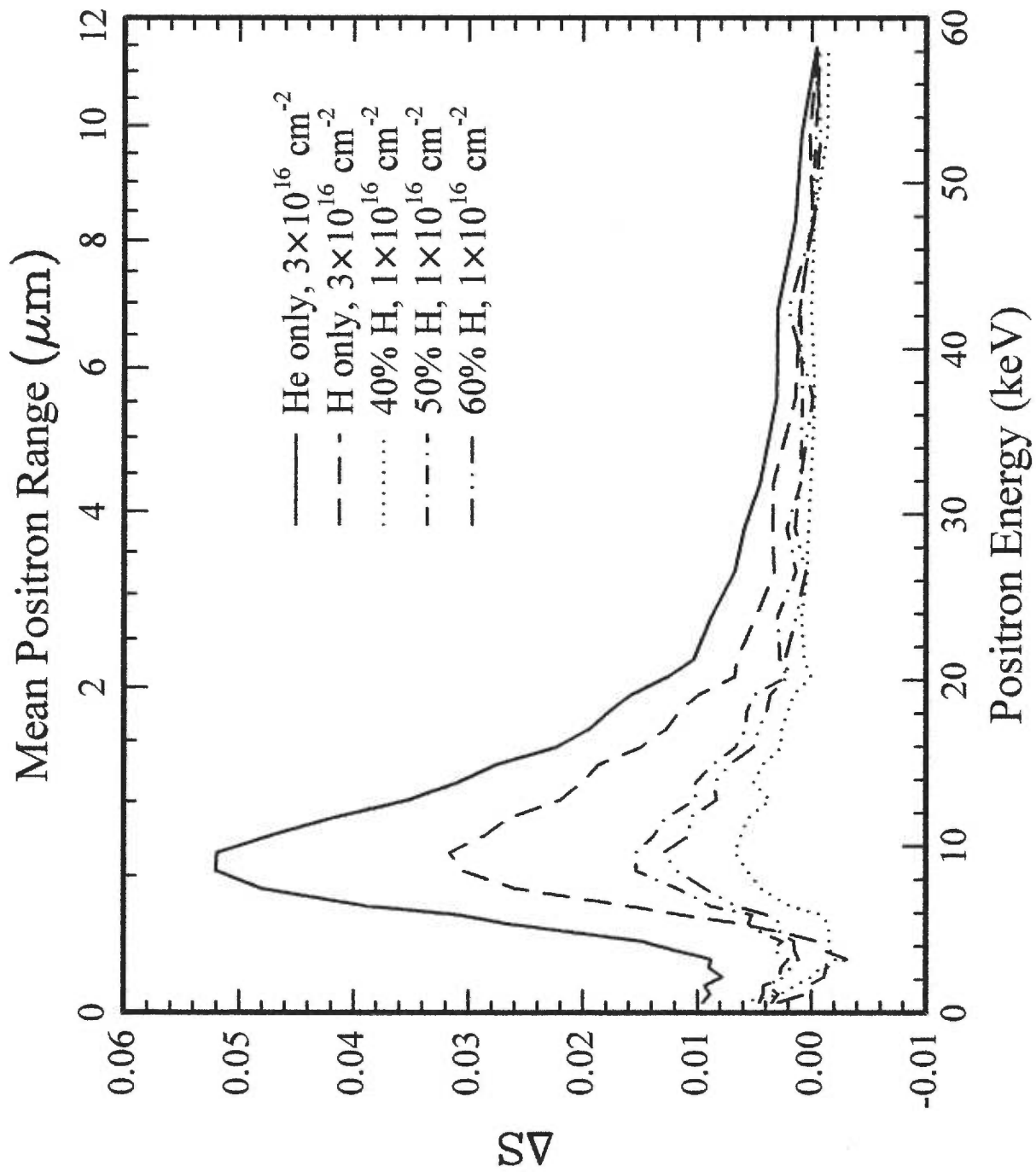
Figure 1

Figure 2

Figure 3

Figure 4

CONCLUSION

En première partie, nous avons tout d'abord confirmé la très grande efficacité des nanocavités comme sites de piégeage d'atomes d'or en mesurant la différence d'énergie libre entre un atome d'Au en solution dans le silicium et un atome adsorbé à la surface d'une cavité. A une température de 800°C, nous avons mesuré une énergie de piégeage de 2,5±0,1 eV. Par comparaison, l'énergie de piégeage d'un atome d'or contenu dans un précipité d'Au-Si est de 2,3 eV. Nous avons également mesuré une différence d'énergie de piégeage de 0,13 eV entre des nanocavités d'un diamètre moyen de 12 nm et des cavités de 34 nm. Cette différence se traduit par une quantité d'or par unité de surface 4,1 fois plus grande à la surface des petites cavités qu'à la surface des grandes. Nous avons proposé que la plus grande courbure des petites cavités est à l'origine d'une diminution de l'énergie d'un atome situé sur cette surface courbe et donc une augmentation de l'énergie de piégeage. Toutefois, la différence théorique due aux effets de courbure et de tension de surface est comprise entre 27 et 59 meV. Les effets de courbure ne semblent donc expliquer qu'en partie l'efficacité accrue des petites cavités. Nous proposons donc également que la densité de sites de piégeage est plus grande à la surface des petites cavités due à des effets de reconstruction plus importants à la surface des grandes. En effet, il est probable que la surface des cavités <10 nm ne subissent pas des effets de reconstruction complexe de type 7×7 bien connue pour inhiber l'adsorption d'or.

En deuxième partie, nous avons démontré que la dose critique nécessaire à la formation de nanocavités dans le silicium peut être abaissée en combinant des implantations d'hydrogène et d'hélium. En utilisant des quantités égales d'hydrogène et d'hélium, la dose totale critique est réduite de 36% comparée à une implantation d'hélium seulement. De plus, la formation de cavités est 42% moins efficace lorsque l'on utilise une implantation d'hydrogène seulement au lieu d'une implantation d'hélium. Par conséquent, la co-implantation permet de diminuer la dose requise de près d'un facteur trois comparée à une implantation d'hydrogène pur. Nous avons aussi montré que l'hydrogène et l'hélium jouent des rôles différents lors de la co-implantation. L'hydrogène passive les liens brisés de silicium créés durant l'implantation tandis que l'hélium diffuse et précipite dans la région défectueuse stabilisée par l'hydrogène en accord avec une espèce chimiquement inerte. Nous proposons finalement un modèle de nucléation de nanobulles, première étape de la formation de nanocavités. Dans ce modèle, l'énergie nécessaire à la création de la surface de la bulle provient du transfert exothermique d'un atome d'hélium en solution dans le silicium vers une phase gazeuse plus stable à l'intérieur de la bulle. L'efficacité de la co-implantation est expliquée par le fait que l'hydrogène diminue l'énergie libre des surfaces des bulles et donc une dose moins grande d'hélium sera nécessaire pour que celles-ci puissent se former dans le silicium.

Finalement, il est à noter que les résultats présentés dans ce travail pourraient être directement utilisés pour optimiser le procédé de fabrication de dispositifs microélectroniques. En effet, la co-implantation permet de restreindre la densité de

défauts introduits dans le substrat lors de la formation d'un système de nanocavités. D'autre part, l'utilisation de cavités de petites tailles (≤10 nm) permet d'augmenter l'efficacité de piégeage de celles-ci et représente donc une technique très efficace pour diminuer les concentrations d'impuretés métalliques dans la région active des dispositifs.

CONTRIBUTION DE L'AUTEUR AUX ARTICLES

Pour le premier article, j'ai effectué la majeure partie des implantations d'hélium et d'or ainsi que la totalité des mesures de spectroscopie par rétrodiffusion de Rutherford (RBS). J'ai également aidé à la préparation et à l'observation des échantillons au microscope électronique à transmission (TEM). J'ai été responsable de la rédaction de la partie expérimentale de l'article et participé à la recherche et l'élaboration des concepts théoriques.

Pour le second article, j'ai été responsable de la préparation de l'expérience, de la prise des mesures expérimentales (à l'exception des mesures PAS effectuées par P. J. Simpson), de la conception du modèle théorique ainsi que de la rédaction de l'article en entier.

REMERCIEMENTS

Je suis très reconnaissant envers mon directeur Sjoerd Roorda pour son support et son encadrement mais aussi pour m'avoir laissé une grande liberté de travail tout au long de mes études de maîtrise. Sa vision à la fois claire, précise et simple de la physique fut également une inspiration pour moi.

Je remercie tout autant François Schiettekatte avec qui j'ai travaillé pendant plus d'un an. François m'a montré tout ce qui peut être fait au laboratoire : de l'utilisation des accélérateurs jusqu'à l'atelier d'usinage en passant par la microscopie optique et électronique. Sa grande débrouillardise, sa facilité à communiquer ainsi que son calme à toute épreuve ont été extrêmement appréciés.

Je remercie également Peter Simpson qui m'a montré que la collaboration avec des chercheurs d'autres universités pouvait se faire facilement et efficacement et être une expérience enrichissante.

Je tiens aussi à remercier mes collègues et amis du département de physique, en particulier : Khalid, Martin, Anna, Rémi et Régis.

Finalement, je remercie Pierre Bérichon (qui prendra bientôt une retraite bien méritée) et Réal Gosselin pour leur soutien technique ainsi que Hélène Lamothe qui a grandement facilité mes démarches administratives.